F. K. Li
M. Leonard Bryan
Jet Propulsion Laboratory
California Institute of Technology
Pasadena, CA 91109

Tradeoffs Among Several Synthetic Aperture Radar Image Quality Parameters: Results of a User Survey Study

The relative importance of parameters for image interpretation is, in decreasing order, resolution, number of multiple looks, and number of bits.

Abstract: *A synthetic aperture radar (SAR) is a complex remote sensor. In such remote sensing systems there are a number of options available for tradeoffs by the system designer. In this study we analyze the effects of adjusting the "number of multiple looks" (i.e., the amount of incoherent averaging used in producing the imagery), the "resolution" (i.e., the spatial distance separating identifiable targets), and the "number of bits" (i.e., the number of quantization levels per sample of the raw SAR signal). Several scenes obtained by the Seasat SAR were processed in a variety of ways and studied by a group of interpreters. Their responses were tabulated with respect to the particular scene and the different processing parameters which were used to produce the images. It is concluded that the relative importance for image interpretation is, in decreasing order, resolution, number of multiple looks, and number of bits. However, these results should not be considered as applicable for all cases, because some observed trends are sharply countered with the nature of the targets imaged.*

Introduction

The imagery obtained by synthetic aperture radars (SAR) have been applied to several remote sensing disciplines such as geologic feature mapping, oceanic phenomena studies, land use and urban morphology studies, etc. (Elachi, 1980; Ford *et al.*, 1980; Beal *et al.*, 1981; Bryan, 1979). The successful SAR experiment on Seasat and the Shuttle (SIR-A) demonstrated the feasibility of global radar mapping at relatively high resolution from a spaceborn platform (Jordan, 1980). It is expected that, in the future, more high quality imagery will be available to the remote sensing community from spaceborne SAR experiments. It is imperative that these future radar systems be designed to meet the users' needs. The purpose of this paper is to examine the requirements of and the tradeoffs among several SAR image quality parameters.

The principle of SAR is well documented (see, for example, Brown and Porcello (1969) and Tomiyasu (1978)). Briefly, high cross-track (range) resolution in a SAR is accomplished by transmitting short, often coded pulses. High along-track (azimuth) resolution is obtained by synthesizing a large antenna aperture with the coherent return received over many pulses. It can be shown that the width of the impulse response in either the range or the azimuth dimension is inversely proportional to the bandwidth of the processed signal in that dimension (see, e.g., Cook and Bernfeld (1968)). Thus, in order to obtain high resolution imagery (i.e., a narrow impulse response width), large bandwidths are required.

The requirements of obtaining high resolution

0099-1112/83/4906-0791$02.25/0
© 1983 American Society of Photogrammetry

imagery pose severe constraints on SAR system designs. For example, high resolution usually requires a large data rate (the data rate for the Seasat SAR was ~110 MBits/s). In the present study, we concentrate on several image quality parameters that are affected by the data rate capacity of a SAR and examine their tradeoffs when the data rate is constrained.

A SAR is a coherent microwave sensor, and the imagery it obtains exhibits "speckle" (also referred to as a "fading" or a "scintillation" effect). The origin of speckle in coherent imaging systems is well described in Dainty (1975). Usually, the presence of speckle is considered detrimental to image interpretation. For example, Kozma and Christiansen (1976) have examined the loss in apparent resolution due to speckle. Another example is the difficulty of making accurate radar backscatter measurements due to the large variations in the pixel intensity. The conventional method to reduce speckle in SAR imagery is through spatial or frequency diversities (Porcello *et al.*, 1976). In these techniques, the available azimuth (spatial diversity) or range (frequency diversity) bandwidths are divided into several portions. Each portion is used to generate an image. Each such image is referred to as a single-look image. The intensities of a pixel in the several images are then averaged. This averaging process reduces the speckle effect (see Dainty (1975)). The average image is referred to as a "multiple-look" image. One must realize that the resolution of a multiple-look image is reduced because the bandwidth used (in range or azimuth) is only a fraction of the full, available bandwidth. In order to maintain the same resolution, the inherent bandwidth of the SAR and the associated data rate must be increased.

Another parameter that affects the required data rate is the number of quantization levels per sample of the raw SAR signal. We will refer to this parameter as the "number of bits" used. We emphasize that the number of bits used for the raw signal is not related to the number of grey levels in the images. Because the SAR signal cannot be used directly as imagery, the effects of the number of bits per sample are different from those of the digitization of the pixel intensities in optical or infrared imagery (such as those obtained by Landsat). Zioli (1975), Wu (1978), and Li *et al.* (1981) have examined the effects of different number of bits used in a SAR. In general, a quasi-uniform background noise is added to the SAR imagery. If the grey level differences of the features under study are relatively small, the presence of this noise may degrade the interpretability of these features.

An important consideration in the design of a SAR system with a limited data rate is the tradeoff among these three image quality parameters: resolution, number of multiple looks, and number of bits per data sample used. Keeping one of these parameters fixed, one can vary the other two parameters in an inverse manner. For example, if the number of bits per data sample is fixed at some value, one can design the SAR system to generate single-look images with resolution of, say, X metres by X metres. The same data rate will allow the SAR system to obtain images with four-looks, $2X$ by $2X$ m resolution or nine-looks, $3X$ by $3X$ m resolution, etc. Another example is the case where the resolution remains fixed. It is then possible to obtain single-look imagery with N bits per data sample, two-look imagery with $(N/2)$ bits per data sample, etc. In fact, the tradeoffs between resolution and number of multiple looks have been examined by Moore (1979), Ford (1981), and Lowry and Hengweld (1980). Moore (1979) has proposed a "spatial-grey-level resolution volume" as an indicator of the optimal number of multiple-looks. This resolution volume is a product of the spatial resolution and the pixel intensity resolution. The pixel intensity resolution improves whereas the spatial resolution deteriorates as the number of multiple looks increases. Moore also presents a curve showing a "figure of merit" versus the number of multiple looks. This curve is reproduced in Figure 1. From this curve, one can see that the optimal number of looks is between two and three, assuming the figure of merit is valid. Furthermore, the curve shows that the figure of merit for a single-look image is approximately the same as that of a ten-look image.

In this paper, the results from a survey study concerning the interpretability of a set of SAR images are presented. The data used to generate these images were obtained by the Seasat SAR experiment. These images span a range of the three image quality parameters. We discuss, in detail, the tradeoffs among the three parameters. The results concerning the tradeoffs between resolution and number of multiple looks support Moore's

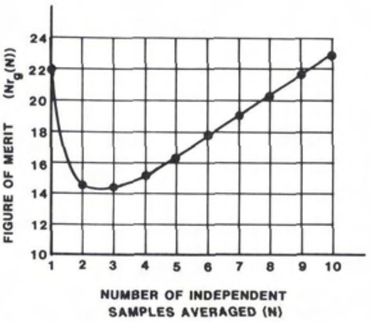

FIG. 1. Figure of merit (defined in Moore (1979)) for processing to different numbers of looks and resolution. Images with a smaller figure of merit are rated better in interpretability in Moore's model.

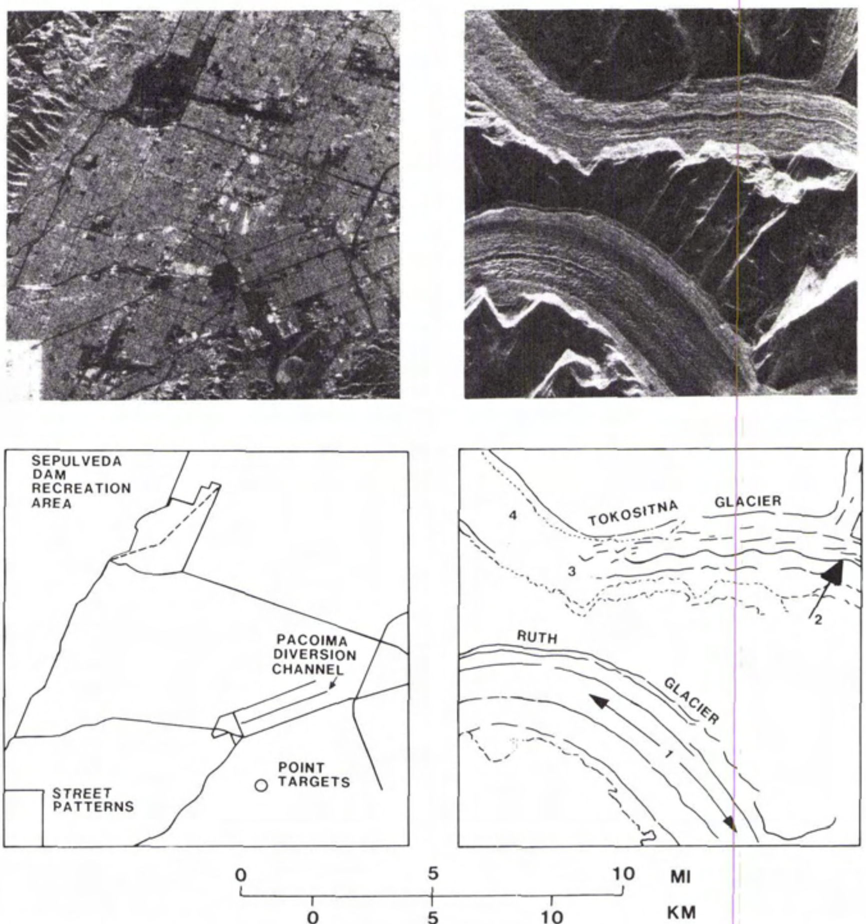

FIG. 2. Standard Seasat digital correlation and sketch maps of the interpretation scenes. Four look, four bit, 25 by 25 m. Left: San Fernando Valley, California. Right: Glaciers in Central Alaska. Radar illumination from top.

model for the cases when the numbers of looks are greater than one. However, the results with single-look imagery do not conform to that model (for details, see below).

IMAGE SCENES AND THE SIMULATION EXPERIMENT

The nominal Seasat SAR imagery has a resolution of ~25 m in range and azimuth with four multiple looks that are obtained by spatial diversity. Thus, the data can be processed into a single look imagery with ~6 m resolution in azimuth and ~25 m resolution in range (Li and Zebker, 1981). The number of bits per data sample was five.

The computer program, described in detail by Li and Zebker (1981), generates the highest resolution, single-look imagery. Images with other resolutions are then obtained by bandpass filtering of the complex, undetected single-look imagery. The resolutions were verified with tests of corner reflectors (see Li and Zebker (1981)). In our study, two different numbers of bits per data sample were used. Each data sample was first truncated to either four or two bits by a computer program. Images were then generated using these truncated data.

Four scenes were chosen for this study; Figures 2 and 3 show the standard Seasat image together with a sketch map of each of these scenes. In both figures the area covered is approximately ~16 by 16 km.

The first scene (Figure 2, left) is of the San Fernando Valley just north of Los Angeles, California. This image was obtained on 21 July 1978, during orbit 351, and is centered at approximately 34° 12′N by 118° 25′W. The features of particular interest for this study, and for which evaluation was requested from the image interpreters, included the set of point targets (rectangular structures), linear features (both the street patterns in the corner and the Pacoima Diversion (drainage) Channels near the center), and an area extensive target, the Sepulveda Dam Recreation Area. The

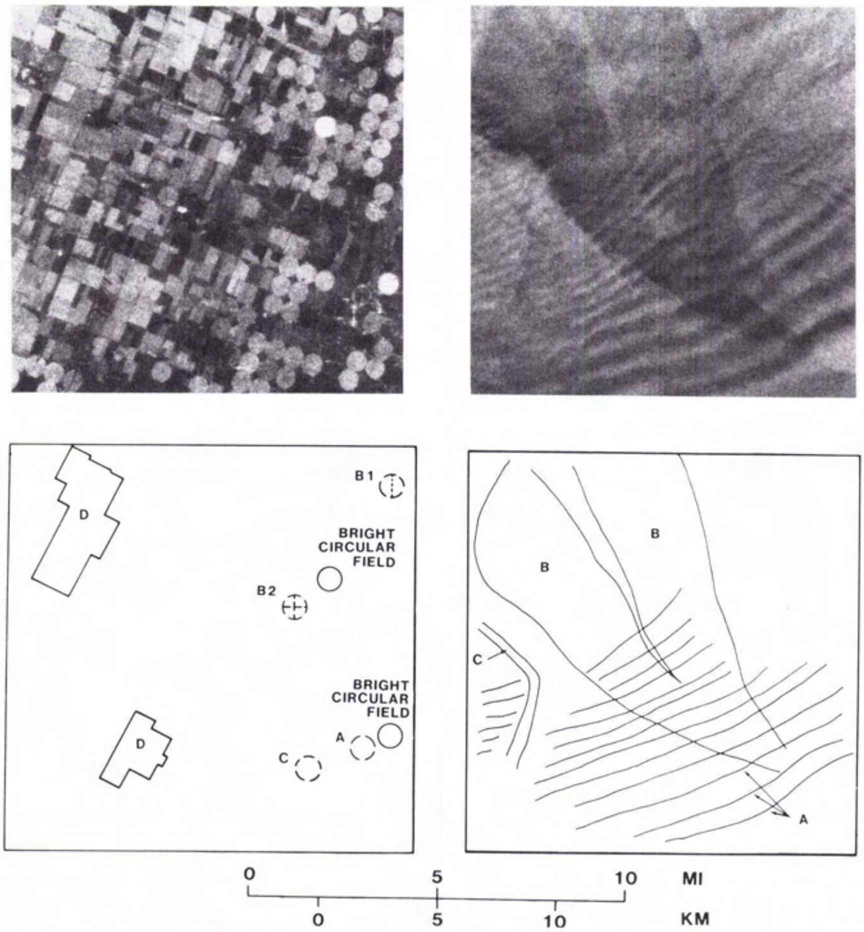

FIG. 3. Standard Seasat digital correlation and sketch maps of the interpretation scenes. Four look, four bit, 25 by 25 m. Left: Agricultural Fields, western Kansas. Right: Ocean Waves in the Gulf of California. Radar illumination from top.

latter is traversed by the linear feature (the Los Angeles River, indicated by the dotted line on the sketch map) and also has numerous quasi-linear rows of diffuse scatterers in the center—these being the rows of trees and "rough" on the golf course within the recreation area.

The second scene is of the Ruth and Tokositna Glaciers in the vicinity of Mt. McKinley, Alaska obtained on 23 July 1978 during orbit 380 (Figure 2, right). These are located at approximately 62° 42′N by 150° 40′W; the glaciers are at elevations of approximately 1800 to 2600 feet (the Ruth Glacier being slightly higher in elevation than the Tokositna) while the interglacial areas are at elevations of 4000 to 4700 feet. Due to the steep relief in this very rugged area, the bright sawtooth expression of the mountains is apparent, as is the layover of the mountains onto the glaciers, especially in the central portion of the Tokositna Glacier. Medial moraines (1) on the Ruth Glacier and (2) on the Tokositna Glacier, terminal moraines (3), and the pitted texture of stagnant ice (4) are the features identified for consideration by the image interpreters.

Scene three (Figure 3, left) is on the very flat and level topography of western Kansas at approximately 37° 47′N by 100° 45′W immediately south of the Arkansas River and approximately 18 km south-east of Garden City, Kansas. The elevation in this area of extensive dry land and irrigated farming averages 2800 to 2850 feet. These data were obtained on 22 September 1978, during Seasat orbit 1254. Item A (Figure 3, left) is a circular irrigated field which has a distinctive bright ring, whereas features B1 and B2 are similar circular fields with definite patterns within the fields themselves. For item C, a dark circular field, and for the areas marked D, fields having tonal patterns which are distinct from the adjacent land are the objects of the image interpreters' efforts. Specifically, the investigations were asked to detect the shape and tones of the features.

The last scene (Figure 3, right) is composed of wave patterns in the area of the Gulf of California approximately 10 miles north-west of the northern tip of the Isla de Angel de la Guardia (approximately 29° 42′N by 113° 45′W). These data were collected on 17 September 1978 during orbit 1183. The patterns identified as "A" are a series of ridge-like wave patterns, probably internal waves. Feature "B" is a wedge-like feature of darker tone and of uncertain origin. The interpreters were requested to identify the ease of distinction of the feature from the adjacent water masses. The same questions were asked concerning a similar, but exceptionally low contrast, feature identified as feature "C."

For each scene, a set of 12 images with different image quality parameters was generated (see Table 1). These parameters were not disclosed to the image interpreters when they were examining the images. Figure 4 shows the 12 simulated images of the San Fernando Valley scene used in this study.

Table 1. Image Processing Parameters*

Image	Number of Looks	Resolution (metres)	Bit Per Sample
A	1	25 × 25	4
B	2	25 × 25	4
C	4	25 × 25	4
D	4	50 × 50	4
E	16	50 × 50	4
F	16	100 × 100	4
G	64	100 × 100	4
H	2	25 × 25	2
I	4	25 × 25	2
J	8	50 × 50	2
K	16	50 × 50	2
L	32	100 × 100	2

* For each of the four scenes studied, a total of 12 digital processings were conducted. This table lists the parameters used in processing each of the 12 images.

The images for each scene were divided into 11 groups (Table 2). The image interpreters were asked to compare the interpretability of the features in the images in each group. For the groups with three images they were asked to select the "best" and the "worst." The remaining image in the group is then assumed to be "medium." For the groups with only two images, the "better" images were selected.

The specific questions concerning the interpretability of the features and the order in which the images were studied by the interpreters are summarized in the Appendix. Several types of feature interpretation were examined: the detection of small, point-like targets, the distinction of grey tone differences, the presence of low contrast features, etc. A total of 27 SAR image users of various levels of experience in radar image interpretation took part in the survey study. Although some of the interpreters had relatively little experience in radar image interpretation, their responses were grouped together as a whole. This is justified for two reasons. First, in another similar radar image interpretation survey concerning geologic features, Ford (1981) has found that the results obtained from the relatively inexperienced image interpreters were substantially the same as those obtained from experienced radar image users. Second, the answers to many questions in our survey were consistent among all interpreters, i.e., a majority (≥80 percent) of the users preferred a particular image over the other images in the same group.

Image Interpretation Survey Results

The results obtained in the survey study are plotted in Figures 5 through 11. For those images considered by the interpreters in groups of three, the number of responses for "best," "medium," and "worst" are plotted for each of the features and for each of the scenes studied. (See Table 2 for the grouping of the images as used during the test.) For those images considered by the interpreters in groups of two, the number of responses for the "better" of the two images is plotted.

Multiple-looks

Figures 5 and 6 present the results of the comparisons of images having the same resolution and the same number of bits per data sample, but with different numbers of multiple looks. A general trend is obvious in these plots wherein the images with increasing numbers of multiple looks are preferred. Image C, with four multiple looks, was almost consistently judged superior to the one-look (A) and the two-look (B) images. As the number of looks increased, the trend continued with 16-look images (Image E, 16 looks, 50 by 50 m, four bit) being overwhelmingly preferred to four-look images (Image D, four-looks, 50 by 50 m, Four bit). This was also noted to be true by the comparison of Image F (16 look, 100 by 100 m, four bit) to Image G (64 look, 100 by 100 m, four bit).

These observations agree with the expectations that, as the speckle is reduced by incoherent averaging, the interpretability of various features improves. It is generally believed that beyond a certain number of multiple looks, additional incoherent averaging does not improve the image interpretability appreciably. This is because the variations in the intensities of the pixels due to speckle have been reduced to a level not discernible by the eyes. However, our results indicate

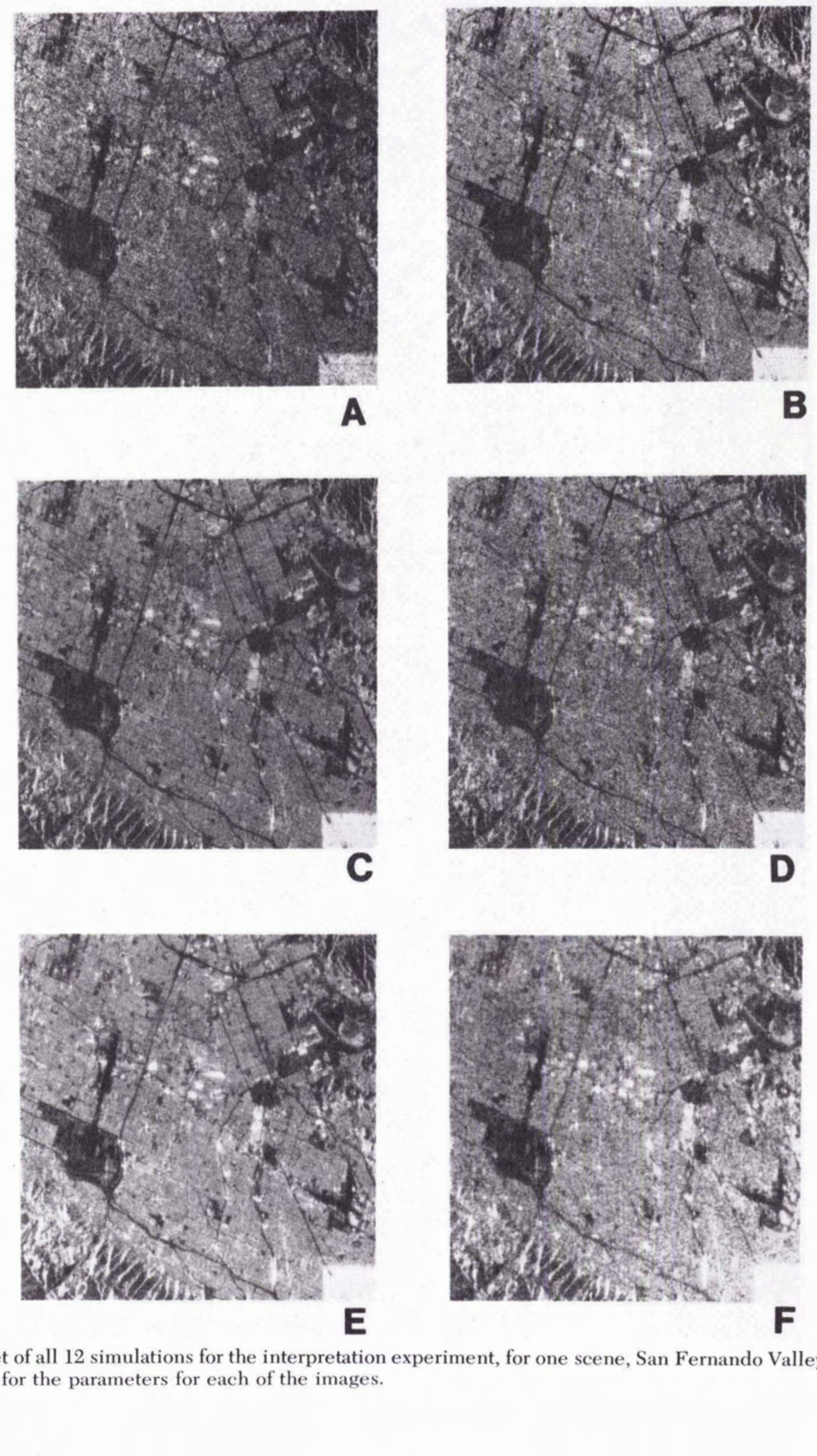

FIG. 4. A set of all 12 simulations for the interpretation experiment, for one scene, San Fernando Valley, California. See Table 1 for the parameters for each of the images.

G

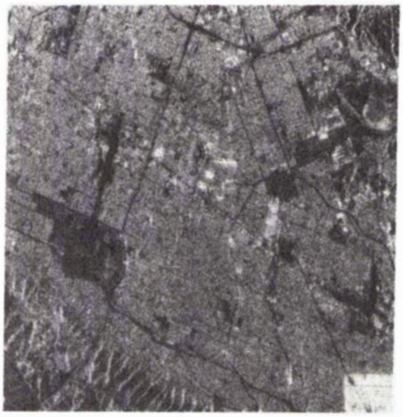

H

I

J

K

L

FIG. 4.—Continued

TABLE 2

Eleven subgroups of images were formed and the images in each group were compared. The groups are:

Image Group	Results Shown in Figures
A vs D vs C	5
D vs E	6
F vs G	6
C vs I	7
E vs K	7
A vs D vs F	8
H vs J vs L	9
C vs E vs G	10
A vs H	11
D vs J	11
F vs L	11

that this level has not been reached for images with 64 looks as compared to those with 16 looks.

This trend of prefering images with larger numbers of multiple looks is obvious in all features examined except for the comparison of feature 1 of scene 2 (medial moraines of Ruth Glacier) and feature 3 of scene 4 (low contrast oceanic features) as shown in Figure 5. Even in these cases, images with the largest number of looks (i.e., four looks) are still preferred, but there is no statistically significant difference between the choices of the one-look and the two-look images. It is possible that in these cases, the reduction in speckle with two multiple looks is still insufficient to improve the interpretability of those features substantially.

NUMBER OF BITS

As mentioned in the introduction, a smaller number of bits per raw data sample generally adds "quantization noise" to the imagery. One might expect that this type of quasi-uniform noise affects mostly the interpretation of relatively dim or low contrast features. Figure 7, therefore, is especially interesting because it shows that the interpretability of almost all the features under study improved when four bits per data sample were used rather than two bits per data sample (Images C and I are 25 by 25 m, four look; Images E and K are 50 by 50 m, 16 look). The presence of the quasi-uniform quantization noise appears to worsen the interpretation of even the brighter targets (e.g., target 2 in scene 1, the street patterns in San Fernando Valley).

NUMBER OF LOOKS VS RESOLUTION

Figures 8, 9, and 10 show the results for the tradeoffs between the number of multiple looks and resolution. In each group, the images were

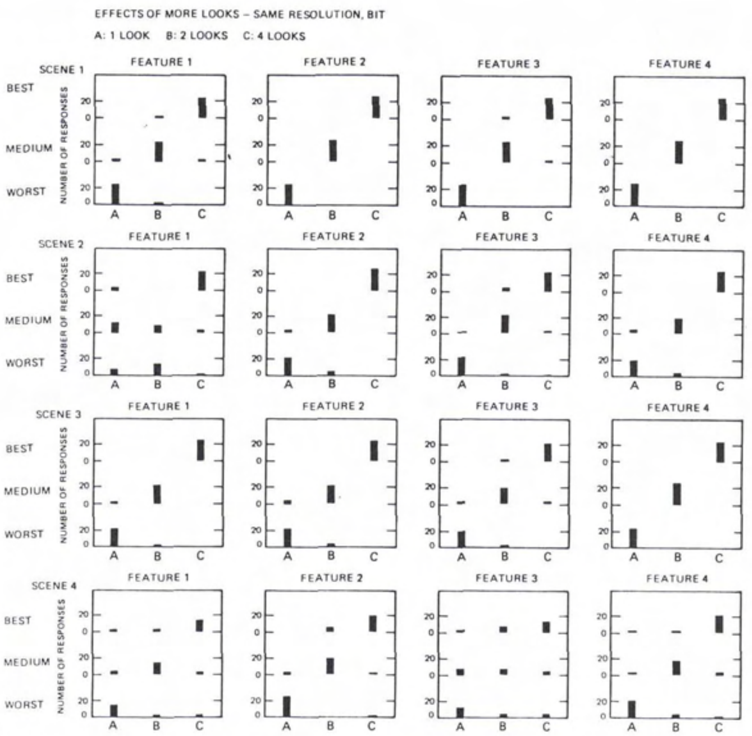

FIG. 5. Results of the interpretations keeping the resolution (25 by 25 m) and number of bits per sample (four) constant; the number of multiple looks varied.

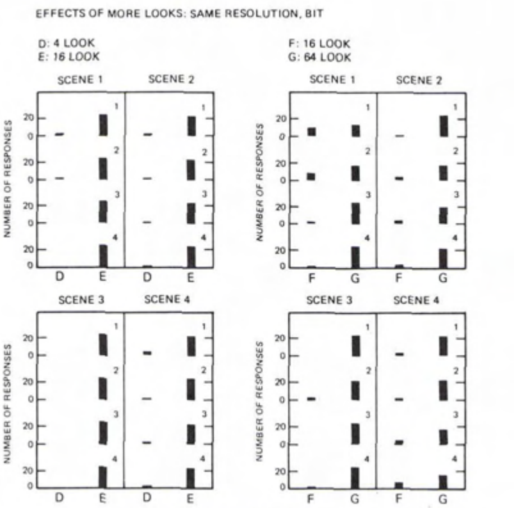

Fig. 6. Results of the interpretations keeping the resolution (25 by 25 m for images D and E; 100 by 100 for images F and G) and the number of bits per sample (four) constant; the number of multiple looks varied. Numbers 1 to 4 for each scene refers to individual features.

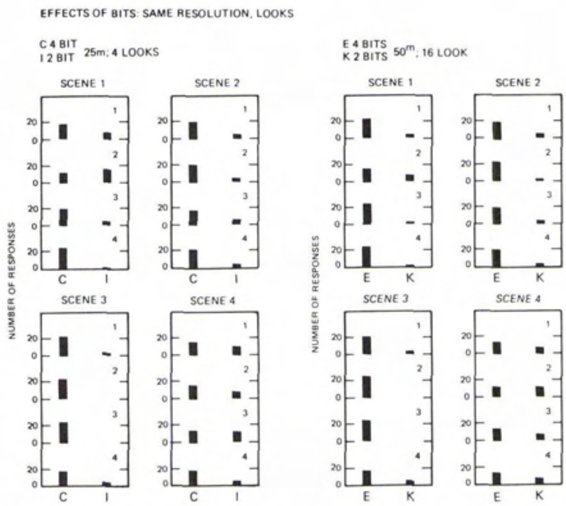

Fig. 7. Results of the interpretation keeping the resolution (25 by 25 m for images C and I; 50 by 50 m for images E and K) and the number of looks (four for images C and I; 16 for images E and K) constant; the number of bits per sample varied. Numbers 1 to 4 for each scene refers to individual features.

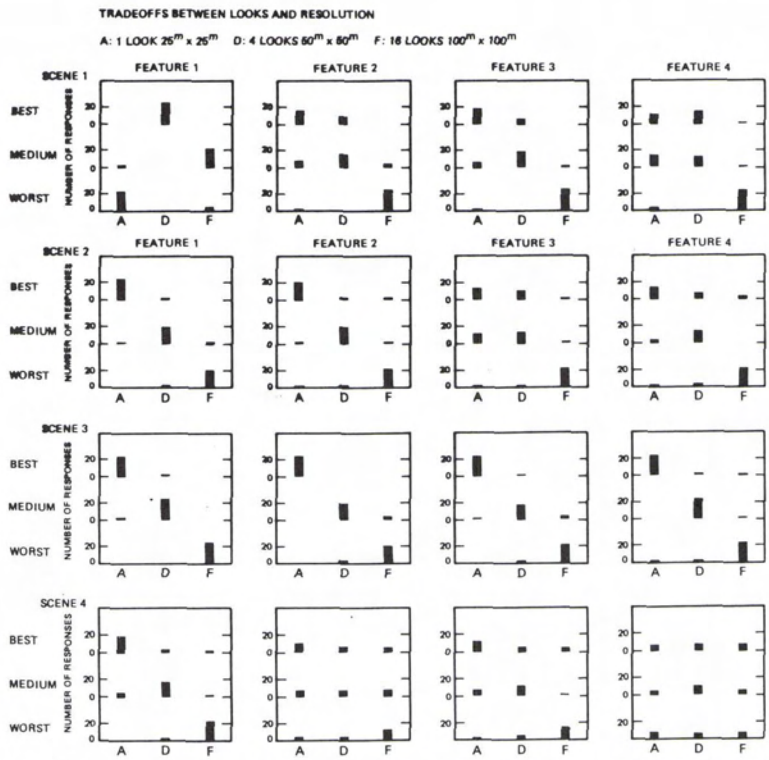

Fig. 8. Results of the interpretations using images with a constant bit rate showing tradeoffs between number of multiple looks and resolution. (A = one look, 25 by 25 m; D = four looks, 50 by 50 m; F = 16 looks, 100 by 100 m.)

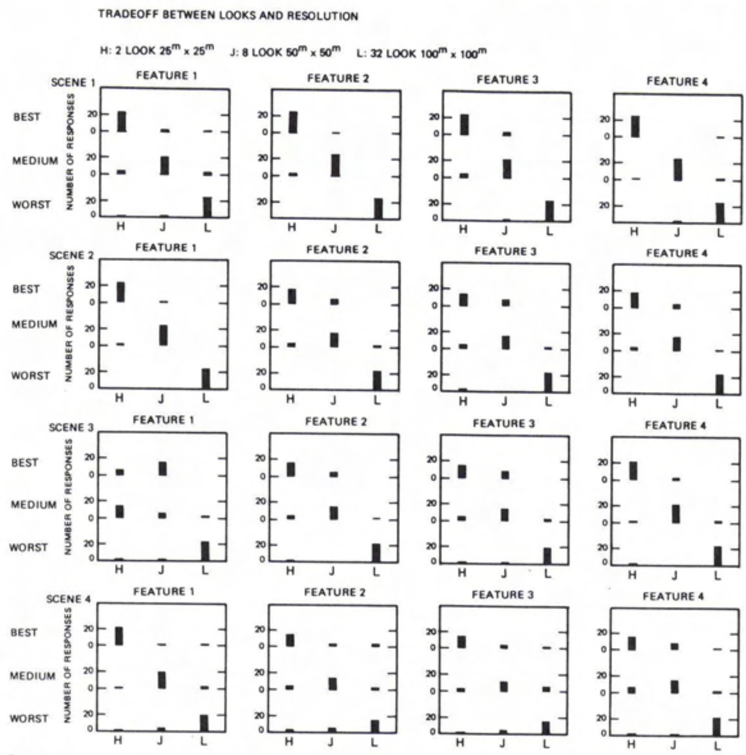

FIG. 9. Results of the interpretation using images with a constant bit rate showing tradeoffs between number of multiple looks and resolution. (H = two looks, 25 by 25 m; J = eight looks, 50 by 50 m; L = 32 looks, 100 by 100 m.)

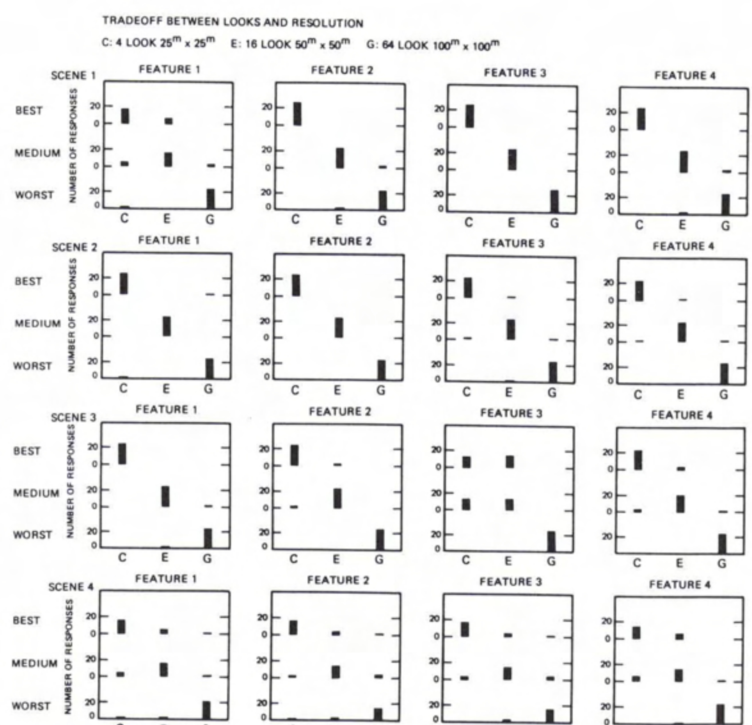

FIG. 10. Results of interpretations using images with a constant bit rate showing tradeoffs between number of multiple looks and resolution. (C = four looks, 25 by 25 m; E = 16 looks, 50 by 50 m; G = 64 looks, 100 by 100 m.)

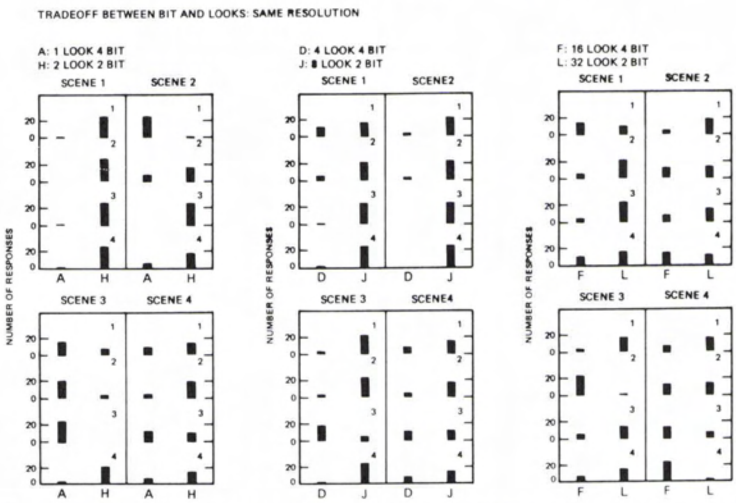

Fig. 11. Results of the interpretations using sets of images with constant resolution and showing tradeoffs between bit rate and number of multiple looks. (A = one look, four bit, 25 by 25 m; H = two looks, two bit, 25 by 25 m.) (D = four looks, four bit, 50 by 50 m; J = eight looks, two bit, 50 by 50 m.) (F = 16 looks, four bit, 100 by 100 m; L = 32 looks, two bit, 100 by 100 m.) Numbers 1 to 4 for each scene refers to individual features.

generated using the same number of bits per data sample (two bits for Figure 9, four bits for Figures 8 and 10), and the number of multiple looks is directly proportional to the area of the resolution element. Thus, in principle, one can obtain the images in each group from SAR systems with the same data rate. A general trend is, again, noted from these plots. Images with the highest resolution (and, therefore, lowest number of looks) are preferred to those with lower resolutions. In fact, for the majority of cases, images with the lowest resolution are rated as worst. The trend is present not only in cases where the features are point or linear targets, but is also present when they are areally extended. Therefore, even in the cases where high resolution is not required to "resolve" the targets, better resolution images are preferred. This trend is also prevalent in the data shown in Figure 8, in which the images have one, four, or 16 looks. These results, therefore, do not conform with the spatial-grey-level resolution volume model of Moore. Two statistically significant exceptions to this trend are feature 1 of scene 1 (rectangular structures in San Fernando Valley) and feature 1 of scene 3 (circular field with bright ring), Figure 9. The first exception is a set of four point-like targets. Examination of the images used by the interpreters shows that these targets were not observable in the image with single-look as compared to the images with two or four looks. This is very likely due to fading (i.e., speckle), which is significant in single look images. When a target under study is areally extensive, it is unlikely that it will become unobservable due to speckle because it is improbable that all the resolution pixels constituting the target would suffer from fading in that particular single look image. When the target concerned is a point-like object, however, it is possible that it is hardly detectable in some single-look images. The second exception to this trend is a circular ring-like feature around a relatively dark field. It is possible that the eight-look image is preferred to the two-look image because the continuity of the ring-like image is more complete in the image with more looks. Further studies of this type of feature is required to fully understand this result.

NUMBER OF BITS VS RESOLUTION

The final set of comparisons (Figure 11) examine the tradeoffs between number of multiple looks and number of bits per data sample used (the resolution is the same within each group). As mentioned above, a smaller number of bits per data sample introduces a quasi-uniform noise level to the images generated. One might expect that this additional noise is not as deleterious as the presence of speckle in the imagery with a small number of looks because of the multiplicative nature of the speckle noise. Indeed, the results shown in Figure 11 generally tend to support this expectation. In many cases, the images with a higher number of looks are preferred to those with a correspondingly higher number of bits per data sample. There are, however, many exceptions to this general trend. It is interesting to note that the preference for a particular feature may change from that of having a larger number of looks to that of having a larger number of bits per data sample. (See, for example, feature 3 of scene 3, a dark circular field in Kansas.) Further studies of these types of features are required to understand the causes for these changes.

Discussion

Although the results reported here are obtained with only a relatively limited data set, they are indicative of several trends in the tradeoffs among the image quality parameters studied. It appears that images with high resolution are preferred to images with lower resolution but larger number of multiple looks (also see Ford (1981)). These results are, therefore, consistent with the spatial-grey-level resolution element model when the number of looks is larger than one. Our data do not agree with this model when single-look imagery is compared with images with a larger number of looks. The curve in Figure 1 indicates that the single-look imagery should rank lower than the four-look imagery with lower resolution. In our results, however, it is the exception rather than the rule that four-look imagery is preferred to single-look imagery. A much more extensive data set covering many different types of targets is required to identify the characteristics of the targets that do not conform to this general trend.

Because the number of bits per data sample appears to be the least important among the three parameters studied, one might consider using only one-bit per data sample and obtain "better" imagery by having either better resolution or a higher number of multiple looks. We caution, however, that when only one-bit per data sample is used, there may be many non-linear effects occurring which will significantly alter the interpretability of the images. Examples of these effects include weak signal suppression, intertarget modulation, loss of low spatial frequency response, etc. (see Li *et al.* (1981) for a discussion of these effects). The presence of these artifacts must be considered in detail.

In addition to the three parameters examined, there are many other image quality parameters that can affect the interpretation of the images, such as side-lobe structure of the impulse response, dynamic range for the images, the spacing of pixels versus the resolution element sizes, etc. Studies on these parameters are being conducted.

Acknowledgments

The authors wish to thank C. Elachi, J. Ford, D. Held, and K. Valente for their aid in the preparation and review of this manuscript. They also thank the many SAR image users who participated in the survey. The research described in this paper was carried out by the Jet Propulsion Laboratory, California Institute of Technology, under contract NAS7-100 with the National Aeronautics and Space Administration.

References

Beal, R. C., P. S. De Leonikus, and I. Katz, 1981. *Spaceborne Synthetic Aperture Radar for Oceanography,* The Johns Hopkins University Press. 1981.

Brown, W. M., and L. J. Porcello, 1969. An Introduction to Synthetic Aperture Radar, *IEEE Spectrum,* V. 6, No. 9, pp. 52-62.

Bryan, M. L., 1979. The Effect of Radar Azimuth Angle on Cultural Data, *Photo. Eng. and Rem. Sens,* V. 45, No. 8, pp. 1097-1107.

Cook, C. E., and M. Bernfeld, 1967. *Radar Signals,* Academic Press, New York, London.

Dainty, J. C., 1975. *Laser Speckle and Related Phenomena,* Springer-Verlag, Berlin, Heidelberg, New York.

Elachi, C., 1980. Spaceborne Imaging Radar: Geologic and Oceanographic Applications, *Science,* Vol. 209, No. 4461, pp. 1073-1082.

Ford, J. P., 1981. *Resolution Versus Speckle Relative to Geologic Interpretability of Spaceborne Radar Images: A Survey of User Reference,* Preprint.

Ford, J., R. Blom, M. Bryan, M. Daily, T. Dixon, C. Elachi, and E. Xenos, 1980. *SEASAT Views North America, the Caribbean, and Western Europe with Imaging Radar,* Pasadena CA, Jet Propulsion Laboratory, Pub. 80-87, 141 p.

Jordan, R., 1980. The SEASAT-A Synthetic Aperture Radar System, *IEEE Journal of Ocean Engineering,* Vol. OE-5, pp. 156-164.

Kozma, A., and C. R. Christensen, 1976. Effects of Speckle on Resolution, *Jour. of the Opt. Soc. of Amer.,* Vol. 66, No. 11, pp. 1257-1260.

Li, F. K., D. Held, B. Huneycutt, and H. Zebker, 1981. Simulation and Studies of Spaceborne Synthetic Aperture Radar Image Quality with Reduced Bit Rate, *Proc. of the 15th International Symposium on Remote Sensing of Environment,* Ann Arbor, Michigan, May 1981.

Li, F. K., and H. Zebker, 1981. A Digital SEASAT SAR Correlation-Simulation Program, *Proc. of the International Geoscience and Remote Sensing Symposium,* Washington, D.C., June, 1981.

Lowry, R. T., and H. G. Hengweld, 1980. "Optimizing Imaging Radar Parameters for Ice Reconnaissance", Presented to the 6th Canadian Symposium on Remote Sensing, Halifax, Nova Scotia.

Moore, R. K., 1979. Tradeoff Between Picture Element Dimensions and Noncoherent Averaging in Side-Looking Airborne Radar, *IEEE Trans. on Aerospace and Elect. Sys.,* V. AES-15, No. 5, pp. 697-708.

Porcello, L., N. Massey, R. Innes, and J. Marks, 1976. Speckle Reduction in Synthetic Aperture Radars, *Jour. of the Opt. Soc. of Amer.,* Vol. 66, No. 11, pp. 1305-1311.

Tomiyasu, K., 1978. Tutorial Review of Synthetic Aperture Radar (SAR) with Applications to Imaging of the Ocean Surface, *Proc. of IEEE,* Vol. 66, No. 5, pp. 563-583.

Wu, C., *Optimal Sampling and Quantization of Synthetic Aperture Radar Signals,* 1978. JPL Publication 78-41, Jet Propulsion Laboratory, California Institute of Technology, Pasadena, California.

Zioli, G. W., 1976. A Lower Bound on the Data Rate for Synthetic Aperture Radar, *IEEE Trans. on Inform. Theory,* Vol. IT-22, pp. 708-715.

(Received 30 April 1982; accepted 28 December 1982; revised 30 January 1983)

Appendix

The questionnaire for the user interpreters is summarized here. For each scene, four features were identified in the sketch maps (see Figures 2 and 3) and the users were asked to compare the images in each group (Table 2) for the interpretability of the features.

Scene 1:

Feature 1. Points targets—in the circle shown there are 4 point-like targets arranged in a line. Detection of these targets.

Feature 2. Street patterns—there is a street pattern shown. These are 4 streets running in a roughly up-down direction with many streets running in a roughly horizontal direction at a closer spacing. Detection of these grid-like patterns.

Feature 3. Diversion Channel—the detection of a relatively bright line (diversion channel) as shown on the diagram.

Feature 4. Features in the Sepulveda Dam Recreation Area—the dotted line in the sketch map marks the Los Angeles River. In area A, there is a golf course which appears as a pattern of narrow, curved features corresponding to the roughs and fairways in the course. Detection of these features.

Scene 2:

Feature 1. Continuity of medial moraines in Ruth Glacier along the section marked by the arrow (number 1).

Feature 2. Clarity of moraines across Tokositna Glacier between arrows (number 2).

Feature 3. The moraines across Tokositna Glacier terminate gradually into stagnant ice. Clarity of moraines situated near this terminus approximately between the arrows.

Feature 4. Pitted texture of stagnant ice on Tokositna Glacier in area marked 4 on the sketch.

Feature 1. Feature A is a circular field with a bright ring-like rim. Detection of this circular ring-like feature and the continuity of the ring.

Feature 2. Features B1 and B2 are circular fields with features inside them. The detection of these features, a vertical feature for B1 and a cross-like feature for B2.

Feature 3. Feature C is a relatively dark circular field. The detection of its circular shape.

Feature 4. Feature D is two areas with many fields. The distinction between fields according to tonal differences.

Feature 1. Feature A is most probably a set of internal waves. Detection of the ridge-like wave-fronts over the whole area sketched.

Feature 2. Distinguish wedge-like feature in Area B which is relatively brighter.

Feature 3. The contrast between Area B and its surroundings.

Feature 4. Feature C is a low-contrast feature. Detection of this feature.

Conference

Renewable Resources Inventories for Monitoring Changes and Trends

Oregon State University, Corvallis, Oregon
15-19 August 1983

Sponsored by the Society of American Foresters, Inventory and Remote Sensing Working Groups; the International Society of Tropical Foresters; the Society for Range Management; the Wildlife Society; the American Society of Photogrammetry; IUFRO, Forest Resource Inventory Subject Group; and the Renewable Natural Resources Foundation; the conference will include technical papers, mini-workshops, and field trips dealing with timely, periodic, and scientifically valid renewable resource inventories.

For further information please contact

Dr. John F. Bell
School of Forestry
Oregon State University
Corvallis, OR 97331